ON-ORBIT PERFORMANCE ANALYSIS OF ULTRASONIC FLOW MEASUREMENT

Yong Chen[1], Xiaohua Gan[1], Xiaoqian Chen[1], Yiyong Huang[1], Bo Yuan[2]

[1]College of Aerospace Science and Engineering, National University of Defense Technology, 410073, Changsha, China.
email: literature.chen@gmail.com

[2]Department of Machinery and Electrical Engineering, Logistical Engineering University, Chongqing, 401311, China.
email: ramboyuanbo@aliyun.com.

On-orbit flow measurement becomes more and more urgent as the on-orbit fluid management shows to be important in the space explorations and operations. Based on the continuous wave propagation, the authors proposes an improved ultrasonic measurement model to easy the configuration and to get a fast response. At 25th, June, 2016, an ultrasonic flow-meter prototype based on the improved model was loaded on CZ-7 rocket which was launched in Wen Chang, China. In the four round on-orbit experiments during the following two days, the flow meter was used to measure the pipeline flow. Meanwhile, the corresponding measurement data have been sent to the ground. Under the prospect that such measurement model may be a trustworthy monitor candidate for future on-orbit fluid management as well as other space operations, present paper concentrates on the introduction of the continuous measurement methodology and analysis of the on-orbit test data.

Keywords: ultrasonic flow measurement, continuous wave propagation, on-orbit experiment, experiment data analysis.

1. Introduction

With the expansion of space explorations and operations, on-orbit fluid management and measurement become more and more urgent and stimulate intensive work on innovative gauging methods during the recent two decades[1, 2]. The applications of propellant on-orbit measurement technology are to detect the end-of-life of satellites, monitor the tank fill level equilibrium and mixture ratio control of bi-propellant systems, resupply a wide variety of fluids to a wide spectrum of on-orbit platforms[3].

On the acknowledgement of the imperative usage requirements of flow meters in the microgravity condition, NASA Lyndon B. Johnson Space Center Propulsion and Power Division performed a flow testing of a wide variety of existed flowmetering concepts to characterize their relative capabilities, limitations, and applicabilities for on-orbit fluid-transfer operations[4]. Under the support of ESA program, Bradford Engineering BV developed an ultrasonic flow meter to measure the propellant consumption during the geostationary transfer phase and during RCT-thruster firing. Such flow meter was qualified for the Chemical Propulsion System of the Alphabus satellite platform which has been launched at July, 2013[1].

Due to the advantages of non-invasive no-moving-parts construction, high potential of bi-directional measurement of rapidly varying flow velocities, and no imposition of any impedance on flow condition, the authors have concentrated on the development of ultrasonic flow measurement technology for on-orbit gauging applications. In the previous work, the authors proposed a measurement model based on continuous wave propagation strategy which is different from the widely used pulse wave strategy[3]. As shown in Chen, et al. [3], the authors used multi-tone wide laning and phase-locked loop methods to solve the intrinsic integral ambiguity problem of the continuous wave configuration. In this paper, the authors improve the previous work to make a faster response and less complicated configurations. Recently, the proposed ultrasonic flow meter was loaded on the CZ-7 rocket which has been launched in Wen Chang, China in 25th, June, 2016. Subsequent on-orbit experiment has been used to test the measurement performance and monitor the real-time pipeline flow condition in the microgravity. The rest of the paper concentrates on the introduction of the improved methodology and the analysis of the on-orbit test data.

2. Improved measurement methodology

Fig. 1 shows the system diagram of ultrasonic flow measurement for microgravity application. Specifically, the ultrasonic wave propagates straightly between two ultrasound transducers which are axially symmetric meanwhile the flow path is diverted 45° (see Yu and Zong [5] for more information) at the entrance and exit of the pipeline. Fig. 2 plots the photogram of the proposed flow meter together with the signal processing electronics and transducers.

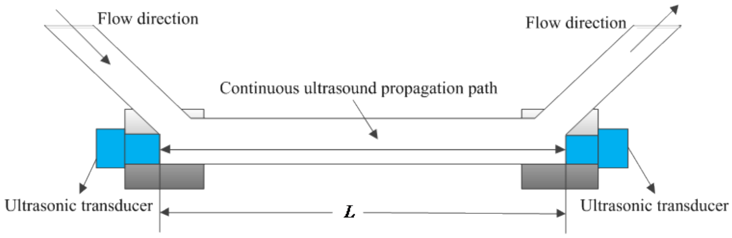

Fig. 1. (Color online) Schematic diagram of proposed ultrasonic flow meter.

It should be noticed that there are many different installation methods existed in industrial applications such as clamp-on scheme. However, as shown by Baird [4], due to the increase of the travel time differences between the upstream and downstream propagation in present configuration, the flow rate calculation is theoretically more accurate. Furthermore, as the upstream and downstream waves are directly received by the transducers without any refraction and reflection, the signal-noise ratio of the received wave is higher compared to other configurations. Thirdly, as the proposed measurement method is established on the continuous wave propagation theory, mathematical analysis turns out to be simple in such configuration. Figure 2 demonstrates the corresponding wave propagation diagram.

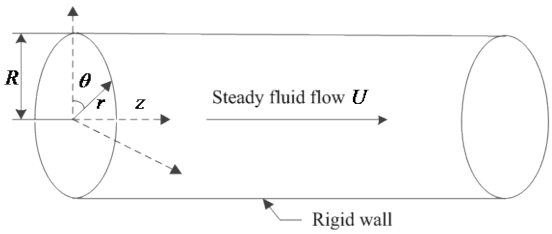

Figure 2. (Color online) Configuration of the wave propagation in circular cylindrical coordinate system (r, θ, and z). R is the pipeline radius with rigid wall, and U is the uniform mean flow profile.

As shown in Figure 2, the pipeline is modeled to be circularly cylindrical with the r, θ, and z denoting the radial, circumferential and axial coordinates respectively. The radius of the pipeline is represented by R meanwhile the fluid is assumed to flow steadily along the rigid-walled pipeline with a uniform mean flow profile U. For a continuous wave propagating along circular cylindrical pipeline, the axially symmetric assumption is reasonable. As a result, the fluid pressure perturbation due to an monochromatic wave propagation can be represented by[3, 6]

$$p' = J_0\left(K_r R r\right)\cdot \exp\left[\mathrm{i}\left(\omega t - k_0 K_z z\right)\right], \tag{1}$$

where K_r, K_z, $\omega\left(=2\pi f\right)$ and $k_0 = \omega/c_0$ are the dimensionless radial wavenumber, dimensionless axial wavenumber, angular acoustic frequency, and the inviscid total wavenumber respectively. The symbol c_0 is the adiabatic sound speed in the unbounded fluid. Under the consideration of fluid's viscothermal effect, the relationship between K_r and K_z is complex as shown by previous research in both liquid[3, 7-12] and gas[13-16]. To make an analytical representation, the following discussion is based on the inviscid fluid assumption. Thus, one can obtain

$$K_r^2 R^2 = k_0^2\left[\left(1-\frac{K_z U}{c_0}\right)^2 - K_z^2\right]. \tag{2}$$

As the pipeline is assumed to be rigid, the radial velocity component of the perturbation vanishes at the wall, which leads to

$$\left.\frac{\partial p'}{\partial r}\right|_{r=1} = 0 \Rightarrow J_1\left(K_r R\right) = 0, \tag{3}$$

showing that the radial wavenumber is independent on the flow velocity. From Eqs. (2) and (3), one can obtain that

$$K_z^{\mathrm{down}} = \frac{-2\pi f U + \left[\left(2\pi f c_0\right)^2 - c_0^2\left(c_0^2 - U^2\right)\left(K_r R\right)^2\right]^{\frac{1}{2}}}{\left(c_0^2 - U^2\right)k_0}, \tag{4}$$

in the downstream propagation and

$$K_z^{\mathrm{up}} = \frac{2\pi f U + \left[\left(2\pi f c_0\right)^2 - c_0^2\left(c_0^2 - U^2\right)\left(K_r R\right)^2\right]^{\frac{1}{2}}}{\left(c_0^2 - U^2\right)k_0}, \tag{5}$$

in the upstream propagation. As show in Figure 1, if the wave propagation path is assumed to be L, the downstream and upstream phases are

$$\Phi_{\mathrm{down}}\left(f\right) = k_0 K_z^{\mathrm{down}} L, \quad \Phi_{\mathrm{up}}\left(f\right) = k_0 K_z^{\mathrm{up}} L. \tag{6}$$

Substituting Eqs. (4)-(5) into (6) yields

$$\Phi_{\mathrm{dif}}\left(f\right) = \Phi_{\mathrm{up}}\left(f\right) - \Phi_{\mathrm{down}}\left(f\right) \approx \frac{4\pi f L U}{c_0^2}, \tag{7}$$

under the assumption of $U^2 \ll c_0^2$ which is acceptable in the flow meter applications. As a result, the volumetric flow Q can be calculated by

$$Q = \pi R^2 U = \frac{\pi R^2 c_0^2}{4\pi f L}\Phi_{\mathrm{dif}}\left(f\right). \tag{8}$$

Thus, one can measure the downstream and upstream phases separately and then calculate the phase difference to predict the volumetric flow. Usually, the values of $\Phi_{\mathrm{down}}\left(f\right)$ and $\Phi_{\mathrm{up}}\left(f\right)$ are larger than 2π which brings the integral ambiguity problem. In the previous work[3], the authors proposed a multi-tone laning strategy to solve the integral ambiguity in the downstream and upstream propagation separately. Specifically, to avoid the integral ambiguity, in both downstream and upstream propagation, the corresponding phase values should be smaller than 2π simultaneously, leading to

$$\Phi_{\mathrm{down}}\left(f\right) < 2\pi, \Phi_{\mathrm{up}}\left(f\right) < 2\pi \Rightarrow \Phi_{\mathrm{down}}\left(f\right) + \Phi_{\mathrm{up}}\left(f\right) < 4\pi. \tag{9}$$

substituting Eqs. (4)and (5) yields

$$\frac{L\left[\left(2\pi f c_0\right)^2 - c_0^2\left(c_0^2 - U^2\right)\left(K_r R\right)^2\right]^{\frac{1}{2}}}{\left(c_0^2 - U^2\right)} < 2\pi. \tag{10}$$

As $U^2 \ll c_0^2$ and $K_r R \gg 0$ according to Eq.(3), one may relax the above requirement to

$$\frac{L\left[\left(2\pi f c_0\right)^2\right]^{\frac{1}{2}}}{c_0^2} < 2\pi \Rightarrow f'_{\min} < \frac{c_0}{L}. \tag{11}$$

On the other hand, the maximum selection of acoustic frequency is related to the measurement precision, which is denoted by $f_{\max}$. In this paper, the calculation of $f_{\max}$ is omitted, readers can consult comprehensive discussion in Ref. [3]. Furthermore, one can decide a set of tones with different frequency to simultaneously handle the integral ambiguity and provide high measurement precision.

In this paper, an improved selection is introduced. Specifically, instead of calculating the phase difference Φ_{dif} at the maximum acoustic frequency $f_{\max}$, one can directly solve the phase difference Φ_{dif} at any frequency using Eq.(7). Under such condition, the minimum frequency which can avoid integral ambiguity is changed to

$$\Phi_{\text{dif}}\left(f\right) \approx \frac{4\pi f L U}{c_0^2} < 2\pi \Rightarrow f''_{\min} < \frac{c_0^2}{2LU}. \tag{12}$$

Clearly, $f''_{\min}$ can be selected to larger than $f'_{\min}$. To give a vivid expression of proposed method's advantage, one can suppose the propagation path is $L = 0.2\text{m}$, the maximum flow velocity $U = 10\ \text{m/s}$, the adiabatic sound speed $c_0 = 1500\,\text{m/s}$. According to Eqs. (11) and (12), one can get

$$f'_{\min} < 7.5\text{KHz},\ f''_{\min} < 562.5\text{KHz}. \tag{13}$$

Thus, one can have the following selection with $f'_{\min} = 2\text{KHz}$ and $f''_{\min} = 200\text{KHz}$, while the maximum frequency is $f_{\max} = 5\,\text{MHz}$. According to Ref. [3], one possible set of tones may be 2KHz, 10KHz, 50KHz, 250KHz, 1MHz, and 5MHz. On the other hand, using the improved method, the set of tones may be 200KHz, 1MHz, and 5MHz. Table 1 and 2 separately gives the phase of two different method using the plane wave mode with $K_r = 0$ as shown in Eqs. (4) and (5).

Table 1. phase value of tones with different frequency in method shown in [3].

Acoustic frequency(KHz)	Phase of downstream propagation with integral ambiguity(°)	Phase of upstream propagation with integral ambiguity(°)	Phase of downstream propagation without integral ambiguity(°)	Phase of upstream propagation without integral ambiguity(°)
2	95.36	96.64	95.36	96.64
10	116.82	123.22	476.82	483.22
50	-135.89	-103.89	2384.1	2416.1
250	40.53	-159.46	11921.53	12080.54
1000	162.12	82.15	47682.12	48322.15
5000	90.59	50.73	238410.59	241610.73

Table 2. phase value of tones with different frequency in the Present's method.

Acoustic frequency(KHz)	Phase with integral ambiguity(°)	Phase without integral ambiguity(°)
200	128	128
1000	-80	640
5000	-40	3200

From table 1, it can be learned that the phase differences of frequency 1MHz and 5MHz are

$$\Phi_{\text{dif}}\left(f = 1\text{MHz}\right) = 640.03^{\text{o}},\ \Phi_{\text{dif}}\left(f = 5\text{MHz}\right) = 3200.1^{\text{o}}, \tag{14}$$

which is consistent with table 2, showing that the improved method is convincible. On the other hand, improved method reduces the number of tones from 6 to 3, which decreases the calculation into half of the previous condition. As a result, the response of the proposed method become faster and the corresponding implementation shows simpler.

3. Data analysis for on-orbit experiment

Using the established measurement model, the authors constructed an ultrasonic flow meter for on-orbit experiment. The ultrasonic flow meter was mounted in the pipeline system where the fluid flowed bi-directionally between two tanks by two pumps. Such experimental instrument was loaded on the CZ-7 rocket launched in Wen Chang, China in 25^{th}, June, 2016. The following subsection concentrates on the measurement performance of the ultrasonic flow meter in the microgravity.

Figure 3 demonstrates the measured instantaneous flow in two different test stages. Meanwhile, the corresponding ground test data have been added which are labeled in green color. In the first stage as shown in the left image, the instantaneous flow vibrates largely which represents that the pump works unsteadily under its start-up stage. With the time increases, the instantaneous flow becomes steady which demonstrates that the pump works in regular condition. Similar phenomenon has been reproduced in the ground test as induced by the ground test data. Careful study illustrates that the instantaneous flow decline quickly as the pump stop work. The fact that the flow data has not any notable vibration demonstrates that the close-down process of the pump is smooth.

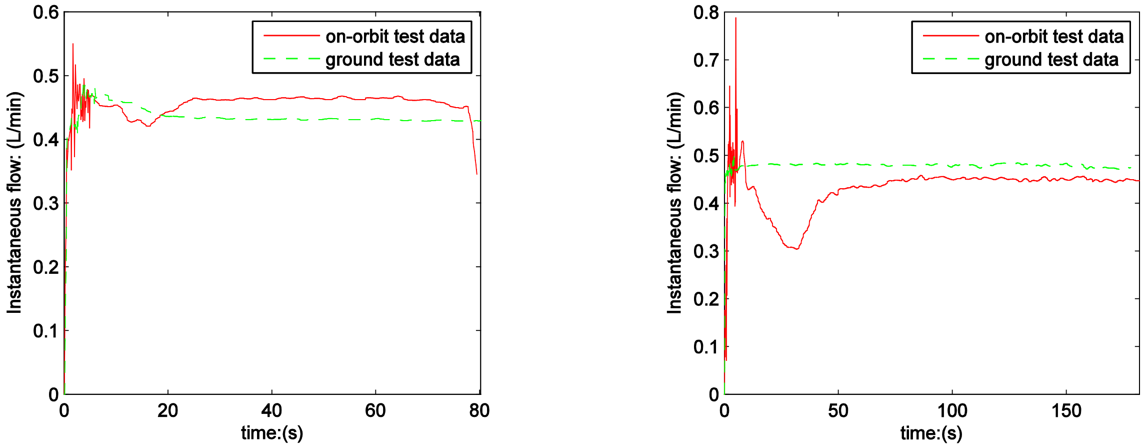

Figure 3(Color online). Comparison of instantaneous measurement performance between on-orbit and ground experimental environments.

In the second test stage shown in the right image, the variation tendency turns to be similar as shown in the first stage. However, the flow in the on-orbit test is smaller than that in the ground test, which is different from that in the first stage. Furthermore, an obvious decrease of the flow demonstrates that the pipeline flow in the micro-gravitational condition is not as steady as that in the gravitational environment. From Figure 3, it can be seen that the variation of the instantaneous flow in the microgravity is more serious than that in the ground which shows that the measurement performance declines in the on-orbit test condition. Table 3 demonstrates the measurement performance of published on-orbit flow measurement devices. It should be noticed that the test accuracy of the proposed ultrasonic flow meter is calculated based on the data as shown in Figure 3.

Table 3. Measurement accuracy of flow meter for microgravity application[1]

Flow meter device	Ground test accuracy	On-orbit test accuracy
Ultrasonic flow meter by Bradford Engineering	0.05% Full scale[1, 2]	Not reported.
Traditional methods like pVT and bookkeeping method	0.6%~2% Full scale[1, 2]	0.6%~2% Full scale
Clamp-on ultrasonic flowmeter by Controlotron	0.25%~1% Full scale[4]	Not reported
Area averaging ultrasonic flowmeter by	1% Full scale[4]	Not reported

Panametrics		
Proposed ultrasonic flow meter	0.007% Full scale	0.01% Full scale

[1]The flow meter range is 0~300 g/s.

In the above table, the full scale of the flow meter is set 300g/s to be consistent with requirement of Alphabus satellite which is a new European telecomminations satellite platform for high payload power ranges[1, 2]. It can be learned that traditional methods like pVT and bookkeeping have the lowest measurement precision while the ultrasonic flow meter turns out to be high precise. From the published paper, ultrasonic flow meters from Bradford Engineering, Controlotron and Panametrics are totally based on the measurement of arrival time of ultrasonic pulses. The ultrasonic flow meter proposed by the authors gives a wonderful measurement performance both in ground and on-orbit tests which experimentally verifies the model's outstanding novelty.

With the help of the ultrasonic flow measurement device, the pipeline flow condition can be monitored simultaneously as shown in Figures 4 and 5. Specifically, Figure 4 illustrates the flow condition in the first test stage when the pump works four times; meanwhile Figure 5 outlines the flow condition in the fourth test stage.

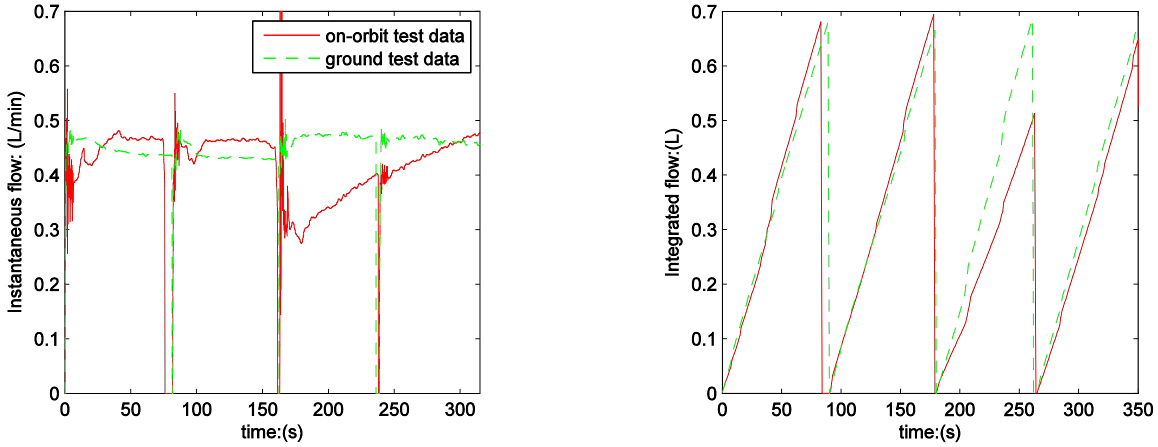

Figure 4 (Color online). Monitor of the flow condition in the first test stage. Left: the instantaneous flow. Right: the corresponding integrated flow. The legend in the right image is the same to that in the left image.

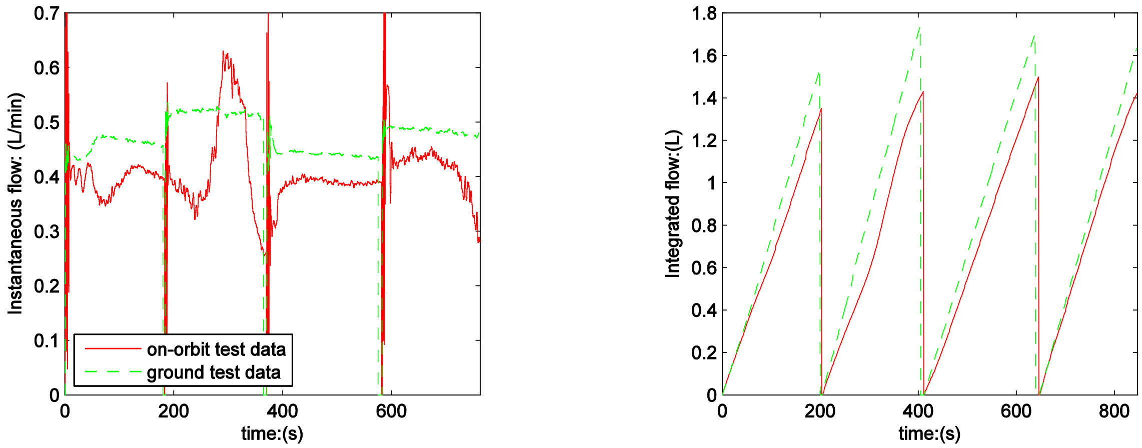

Figure 5(Color online). Monitor of the flow condition in the fourth test stage. Left: the instantaneous flow data. Right: the corresponding integrated flow data. The legend in the right image is the same to that in the left image.

The flow condition in Figure 4 shows steadier than that in Figure 5 which means that the pipeline flow condition becomes more and more unsteady as the on-orbit experiment goes on. The on-orbit transport volumes of the liquid in the first two times keep consistent with the ground test data as shown in Figure 4. For the rest of the on-orbit test, the on-orbit transport volumes are smaller than those in the ground test. Furthermore, the condition of fluid flow becomes more and more unsteady as the vibration of the instantaneous flow data becomes more and more obvious which has been shown in the left image of Figure 5. The integrated flow data represent the resupplied fluid from one tank to another tank. Using the integrated data, one can easily calculate the tank fill level equilibrium.

4. Conclusion

In summary, based on previous research, present paper proposes an improved continuous ultrasonic flow measurement model to easy the configuration of flow meter and to get a faster response. With the aid of CZ-7 rocket, its measurement performance has been verified in the microgravity. Experimental data shows that the flow meter has an outstanding measurement precision with 0.01% full scale on-orbit test error and 0.007% full scale ground test error. Such device can be used to monitor the instantaneous flow condition as well as the integrated flow, which will be a prominent tool for the detection of satellite’s end-of-life and management of on-orbit propellant in the future task.

The work described in this paper is funded by the National Natural Science Foundation of China(No. 11404405, 11504427, 61601489, and 51675525), the Major Program of National Natural Science Foundation of China (No. 61690210 and 61690213) and by the National Innovation Training Project of Undergraduate Student(No. 20169002001). The authors gratefully acknowledge the funding.

REFERENCES

1 Matthijsen, R. and Put, P. V. Ultrasonic flow meter for satellite propellant gauging and ground test facilities, *44th AIAA/ASME/SAE/ASEE Joint Propulsion Conference & Exhibit*, (2008).

2 Matthijsen, R. and Put, P. V. "State-of-the art" gauging components for improved propellant management on 3-axis stabilized spacecraft, *42nd AIAA/ASME/SAE/ASEE Joint Propulsion Conference & Exhibit* (2006).

3 Chen, Y., Huang, Y. and Chen, X. Acoustic propagation in viscous fluid with uniform flow and a novel design methodology for ultrasonic flow meter, *Ultrasonics*, **53**, 595-606, (2013).

4 Baird, R. S., Report TM-100465, Flowmeter evaluation for on-orbit operations, (1988).

5 Yu, Y. and Zong, G. Ultrasonic liquid flow meter for small pipes, *Review of Scientific Instruments*, **83**, 026107, (2012).

6 Willatzen, M. Flow acoustics modelling and implications for ultrasonic flow measurement based on the transit-time method, *Ultrasonics*, **41**, 805-810, (2004).

7 Chen, Y., Huang, Y. and Chen, X. Thermal-mechanical flow acoustics in inviscid non-uniform shear flow confined by heating pipeline and implications for ultrasonic flow meter, *Acta Acustica United with Acustica*, **99** (4), 503-513, (2013).

8 Chen, Y., Huang, Y. and Chen, X. Ultrasonic wave propagation in thermoviscous moving fluid confined by heating pipeline and flow measurement performance, *Journal of the Acoustical Society of America*, **134** (3), 1863-1874, (2013).

9 Chen, Y., Huang, Y. and Chen, X. Isentropic acoustic propagation in a viscous fluid with uniform circular pipeline flow, *Journal of the Acoustical Society of America*, **134** (4), 2619-2622, (2013).

10 Chen, Y., Huang, Y. and Chen, X. Viscothermal longitudinal wave propagation in non-uniform shear liquid flow confined by constant temperature pipeline and implications for ultrasonic flow meter, *Acta Acustica United with Acustica*, **99** (6), 875-890, (2013).

11 Chen, Y., Huang, Y., Chen, X. and Bai, Y. Isentropic wave propagation in viscous fluid with uniform flow confined by lined pipeline, *Journal of the Acoustical Society of America*, **136** (4), 1692–1701, (2014).

12 Chen, Y., Huang, Y., Chen, X., Bai, Y. and Tan, X. Isentropic wave propagation in a viscous fluid moving along a lined duct with shear flow and its implication for ultrasonic flow measurement, *Aerospace Science and Technology*, **39**, 72-85, (2014).

13 Chen, Y., Huang, Y., Chen, X. and Hu, D. Axisymmetric wave propagation in uniform gas flow confined by rigid-walled pipeline, *Journal of Computational Acoustics*, **22** (4), 1450014, (2014).
14 Chen, Y., Huang, Y., Chen, X., Bai, Y. and Tan, X. Axisymmetric wave propagation in gas shear flow confined by a rigid-walled pipeline, *Chinese Physics B*, **24** (4), 044301, (2015).
15 Chen, Y., Chen, X., Huang, Y., Bai, Y., Hu, D. and Fei, S. Study of thermoviscous dissipation on axisymmetric wave propagating in a shear pipeline flow confined by rigid wall. Part I. Theoretical formulation, *Acoustical Physics*, **62** (1), 27-37, (2016).
16 Chen, X., Chen, Y., Huang, Y., Bai, Y., Hu, D. and Fei, S. Study of thermoviscous dissipation on axisymmetric wave propagating in a shear pipeline flow confined by rigid wall. Part II. Numerical study, *Acoustical Physics*, **62** (2), 143-150, (2016).